Amigó, V.; Salvador Moya, MD.; Romero, F.; Solves-Camallonga, C.; Moreno, J. (2003). Microstructural evolution of Ti-6Al-4V during the sintering of microspheres of Ti for orthopedic implants. Journal of Materials Processing Technology. 141(1):117-122. https://doi.org/10.1016/S0924-0136(03)00243-7

Microstructural evolution of Ti–6Al–4V during the sintering of microspheres of Ti for orthopedic implants

V. Amigó[1], M.D. Salvador[1], F. Romero[1], C. Solves[1,2], J.F. Moreno[2]

[1] *Dept. d'Enginyeria Mec I de Mater., Universidad Politécnica de Valencia, Camino de Versa s/n, Valencia 46022, Spain*

[2] *Bio-Vac España, S.A., Benjamin Franklin 25, Parque Tecnologico, Paterna, Valencia 46980, Spain*

Abstract

The sintering of microspheres for porous coating is made in titanium alloys at temperatures close to 1400 °C, thus substantially modifying the microstructure of the bases alloy. This changes is fundamentally due to grain size enlargement and α + β Widmanstaetten structure.

Therefore it is necessary to make a deep study of grain growth effect on the hardness of the base material and the component of the sintered balls, in order to evaluate mechanical properties variation due to changes in the microstructure.

There are also important complementary stabilization treatments of the microstructure by means of controlled cooling at high speeds it avoids the formation of β phases in grain boundaries, at the same time that avoid the broken-up of the Widmanstaetten structure, developing in an increase in mechanical resistance and fatigue resistance of the prosthesis.

***Keywords**:* Titanium alloys; Porous coating; Microstructure; Sintering

Introduction

Ti–6Al–4V, according to ASTM F-136 and ISO-5832-3, is one of the metallic biomaterials actually used. One of its main uses is the hip and knee prosthesis due to its mechanical properties and its excellent corrosion behaviour. Forging processes can be used to obtain first shapes of the implants.

Fixation of joint replacement prosthesis is a necessary requirement for a successful performance of these implants. The concept of biological fixing of the prosthesis by bone ingrowth rather than cemented prosthesis has evolved in an attempt to decrease the incidence of loosening [1]. The attractive of biological fixation lies in its direct attachment of the implant to bone without an interposed layer [2].

Porous coating of surgical implants for their fixation by bone ingrowth (osteo-integration) into a three-dimensional matrix of interconnected porosity has given good clinical results. The evidence of bone ingrowth has been studied [3,4] as well as the optimum pore size has been evaluated [5]. The most used surface for bone ingrowth is the beads sintered coating [6,7]. Commercially pure titanium (CPTi) or Ti–6Al–4V beads, diameters from 250 to 650 μm to provide pore size from 150 to 250 μm, are attached to the titanium alloy prosthesis in different number of layers, from one up to four [4].

The prosthesis, with the beads coating initially glued, are thermally treated in a controlled atmosphere furnace to form bonds between the beads and the substrate as well as between the beads themselves. These bonds, necks, are about 30–35% of the bead diameter, thus providing a porosity of 35–40%. The process of sintering beads to a substrate necessitates thermal exposures at about 1400 °C (over b-transus temperature) for 5–7 h, cause microstruc- tural changes that may have effects on the mechanical properties of the alloy [8,9].

Experimental procedure

Materials

This investigation was developed in Ti–6Al–4V femoral stem of hip implants (Fig. 1) supplied by Thorton Precision Components Forging Company, Sheffield, UK, whose ana- lytical spectrum is shown in Fig. 2.

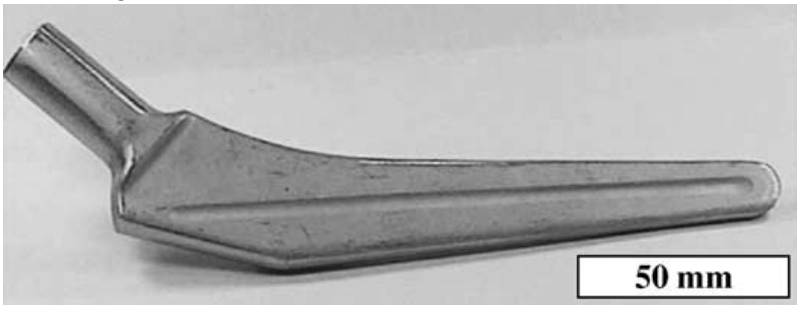

Fig. 1. The femoral stem of hip implant, as forged.

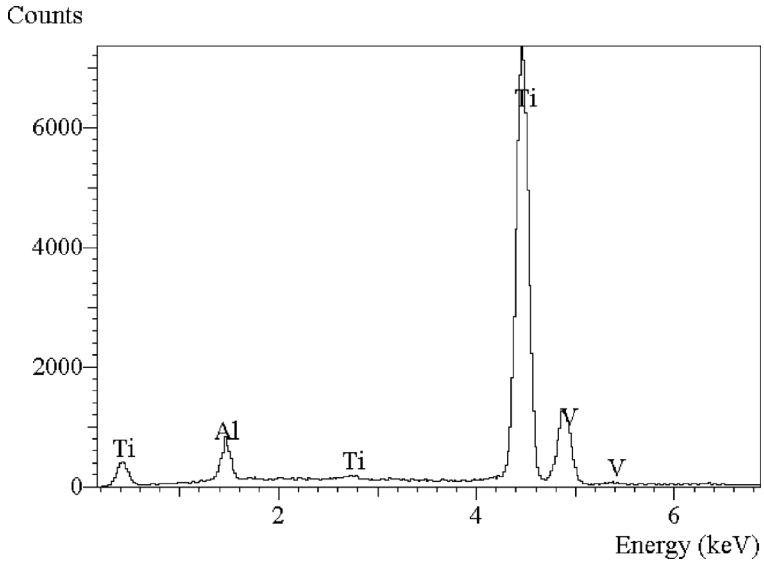

Fig. 2. Dispersive energy spectrum of the forging implant component.

Chemical composition is given in Table 1 and mechanical properties are given in Table 2. The pieces comply with ASTM F-136 [10] and ISO-5832-3 standards [11].

Beads of unalloyed Ti powder, according to ASTM F- 1580 standard [12], were used. The beads were produced by centrifugal atomisation to obtain a high purity powder, and plasma rotating electrode process (PREP) was chosen to avoid contamination from the stationary electrode and have been supplied by Starmet Corporation, MA, USA. The chemical composition of the beads complies with ASTM F-1580 and matches with CPTi grade II of ASTM F-67

standard [13]. Chemical composition is given in Table 3. All the beads produced were screened in meshes to separate the needed diameters. The average size of the beads was 307 mm (mesh -45 to þ60). The size distribution is given in Table 4.

Table 1. Implant forging chemical composition

Element	Implant analysis (%)	ASTM F-136 (%)	ISO 5832-3 (%)
Aluminium	5.89	5.5–6.5	5.5–6.5
Vanadium	3.84	3.5–4.5	3.5–4.5
Nitrogen	0.009	0.05 (max.)	0.05 (max.)
Carbon	0.014	0.08 (max.)	0.08 (max.)
Hydrogen	0.0006	0.012 (max.)	0.015 (max.)
Iron	0.09	0.25 (max.)	0.3 (max.)
Oxygen	0.11	0.13 (max.)	0.2 (max.)
Titanium	Balance	Balance	Balance

Table 2. Implant forging mechanical properties

Property	Implant analysis	ASTM F-136	ISO 5832-3
Tensile strength (MPa)	922	860 (min.)	860 (min.)
Yield strength (MPa)	843	795 (min.)	780 (min.)
Elongation (%)	16	10 (min.)	10 (min.)
Reduction of area (%)	47.8	25 (min.)	25 (min.)

Table 3. Beads before sintering chemical composition

Element	Beads analysis (%)	ASTM F-1580 (max.%)
Nitrogen	0.009	0.05
Carbon	0.02	0.10
Hydrogen	0.002	0.05
Iron	0.14	0.50
Oxygen	0.18	0.40
Silica	0.01	0.04
Chlorine	0.001	0.20
Sodium	<0.0005	0.19
Titanium	Balance	Balance

Table 4. Bead size distribution

Mesh (US series)	Opening (mm)	Retained on screen (%)	Finer than this size (%)
40	420	0.0	100.0

45	350	2.3	97.7
50	297	60.0	37.7
60	250	36.4	1.3
70	210	1.3	0.0

Sintering process and ulterior heat treatments

The implant was coated with three layers of beads. The beads were attached to the implant using a binder. The implant coated was thermally treated in a vacuum furnace. The sintering process was 1400 °C during 6 h followed by a furnace cooling. After the sintering process, the material can undergo solution treatment and aging (STA) or broken-up structure (BUS).

Solution step is at 1025 °C (close to β-transus) during 30 min, followed by fast cooling, using argon as quenching gas; during the aging step, the pieces are kept at temperatures ranged from 620 to 850 °C, where times range from 2 to 8 h. These thermal treatments provoke a grain size enlargement.

Microstructure characterisation

To study the evolution of the microstructure of the alloy during the sintering process, samples were metallographic prepared by conventional techniques. Specimens surfaces were etched with Kroll's reagent (3 cm^3 of HF and 6 cm^3 of HNO_3 in 100 ml of H_2O). Microstructure observations were made by optical microscopy (Nikon Microphot FX) and scanning electron microscopy (JEOL 6300) with X-ray microanalysis (Link Isis EDX). With these techniques it was possible to determine the components variation between the bulk and the precipitate particles.

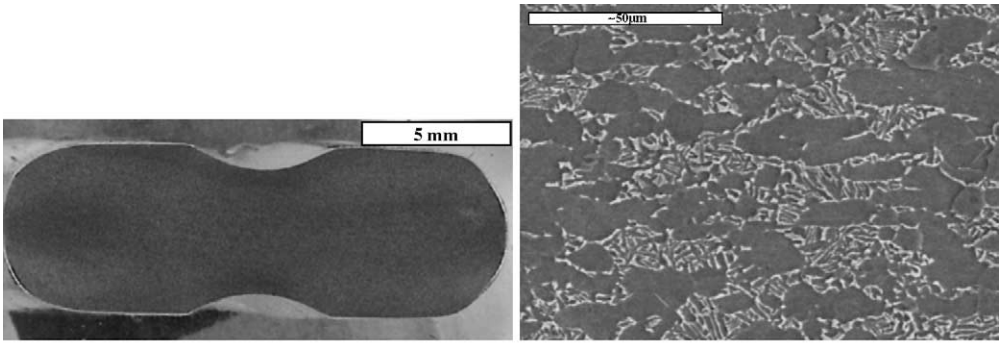

Fig. 3. (a) Macrography of the section of the implant, mill-annealed. (b) Microstructure of the implant, mill-annealed, by SEM (Kroll reagent etching).

Results and discussion

Wrought material forged, Fig. 3 shows a typical mill-annealed microstructure, which is composed of finely dispersed β particles in a fine equiaxial grain matrix of α.

The image of the beads is shown in Fig. 4a and detail of its surface is shown in b and c, where the solidification surface of the material can be appreciated. Solidification microstructure of the beads is shown in d, where no significant solidification contraction or solidification cracks are observed.

The sintered material shows a lamellar structure of coarse plates of a and b, due to the slow cooling rate. The grain size has been enlarged due to the long time at high temperature. There is a significant difference in the grain size from the external side (3–4 mm) of the stem to the internal core. Internal grains (Fig. 5d) are quite bigger than external grains (Fig. 5c). The grain growth does not take place in a uniform way in the whole specimen. It seems that the grain growth kinetics of the alloy does not follow the Hillert distribution of sizes, since the maximum radius is bigger than 1.8 times the value of the average radius.

α-Phase has precipitated in some of the grain boundaries, this grain boundary a is characterised by straight lines of β that separates a from the rest of the matrix (Figs. 5d, 6a and b). This phenomena is critical in bonding between the microspheres and the implant (Fig. 6a and b) as it enbrittles this low section area. α-Plates can also create a notch effect where the plate arrives to the surface of the material.

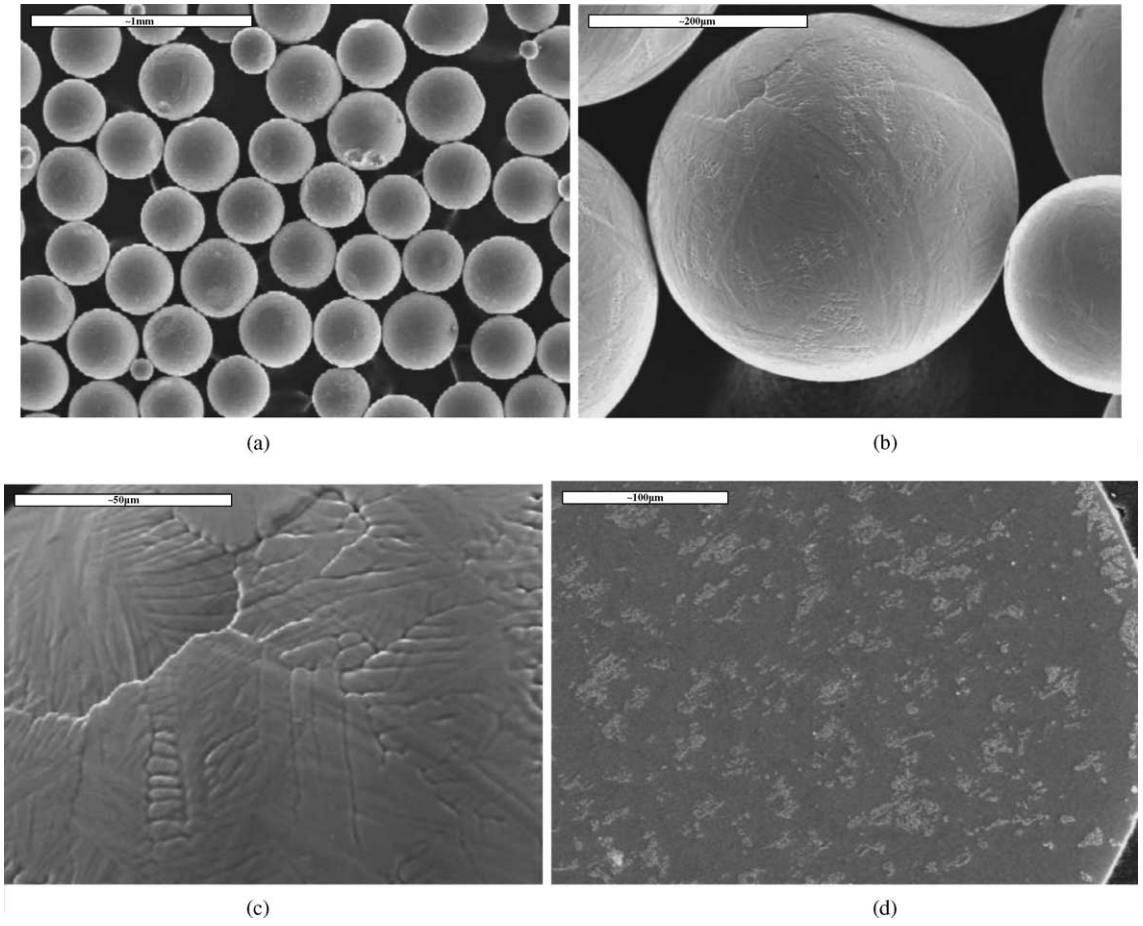

Fig. 4. (a) SEM image of the beads, (b and c) solidification surface of the beads, and (d) microstructure of the beads: no significant solidification contraction or solidification cracks are observed.

Fig. 5. (a) The femoral stem of hip implant, with the sintered coatings. (b) Macrography of the

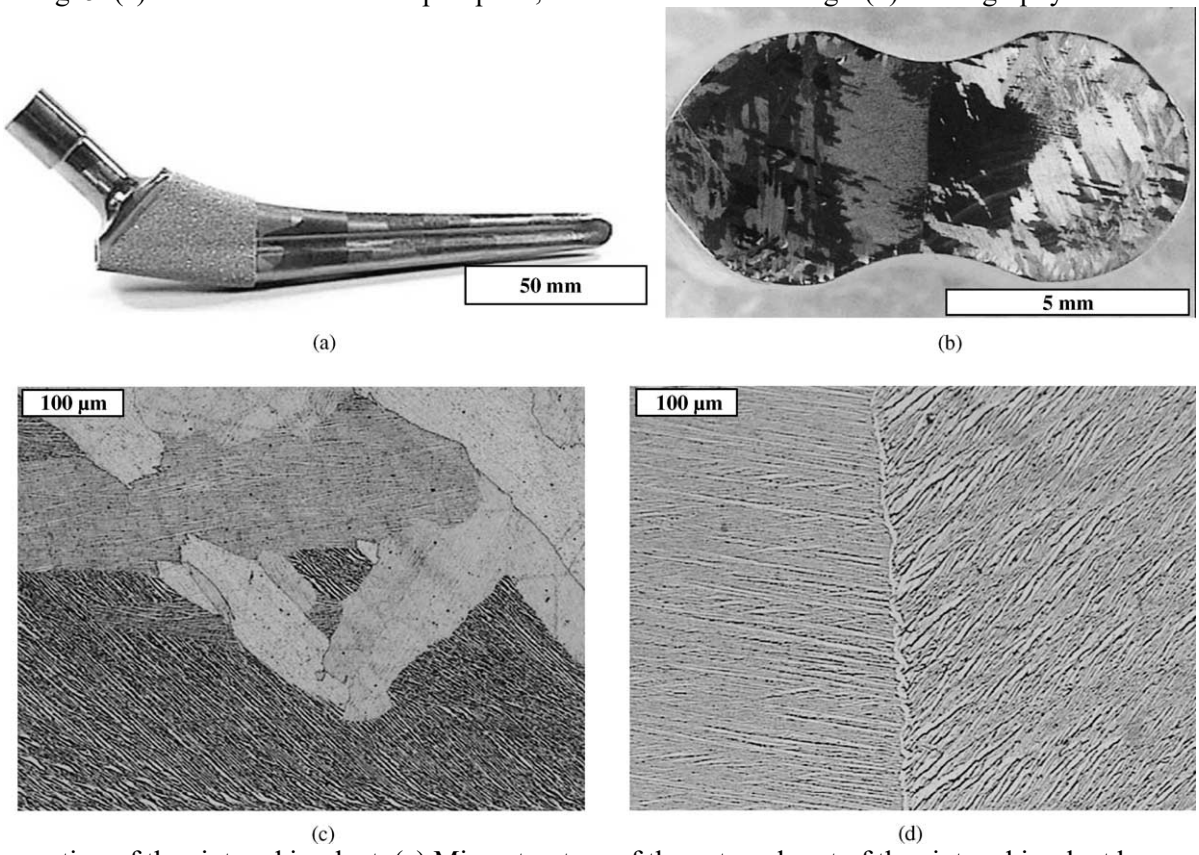

section of the sintered implant. (c) Microstructure of the external part of the sintered implant by SEM (Kroll's reagent etching). (d) Microstructure of the internal part of the sintered implant; same technique, same etching.

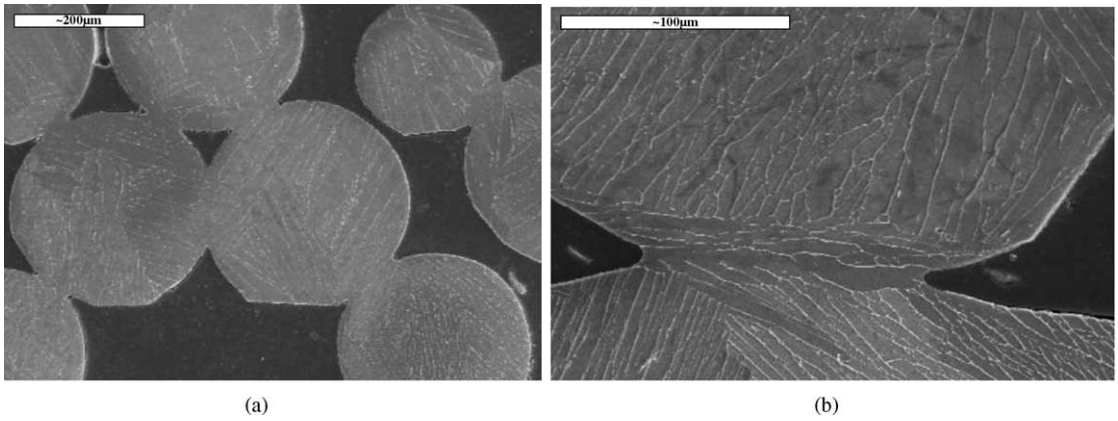

Fig. 6. Microstructure of the bonding between the microspheres (a) by SEM (Kroll's reagent etching) and (b) the implant; same technique, same etching.

After post-sintering BUS treatment the microstructure shows an acicular structure (Fig. 7). A martensitic-type transformation breaks the Widmastaetten plates into fine acicular shapes.

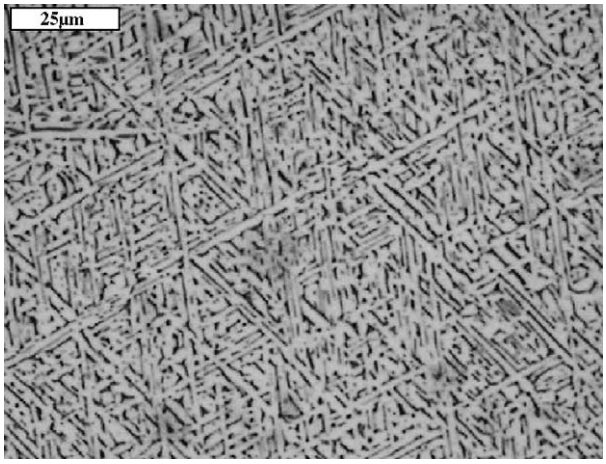

Fig. 7. Microstructure of the implant, BUS treated (Kroll's reagent etching).

Mechanical properties after sintering treatment (yield strength 788 MPa) are minor than previous mechanical properties, those that material exhibited just after forging and mill annealing (yield strength 843 MPa). The yield strength cannot be improved by BUS thermal treatment.

Nonetheless, microhardness (Fig. 8) does not shows this decreases due to the fact that lamellar microstructure is similar on all cases. Microhardness just after forging and mill annealing was 359 HV. After sintering treatment it was 378 HV in the medium size external grains and 476 HV in the large internal grains.

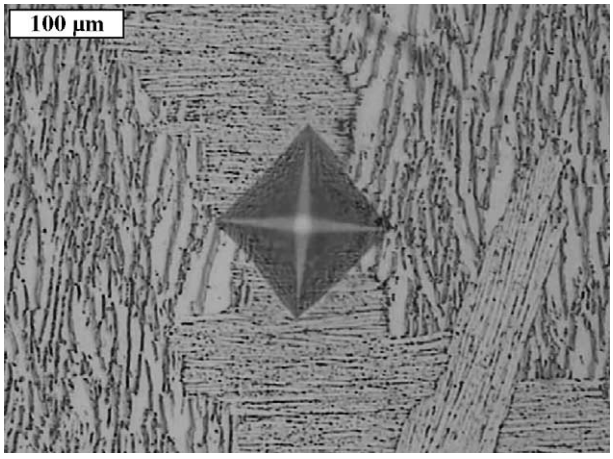

Fig. 8. Microstructure of the medium size external grains with Vickers microhardness mark.

The plasticity of the lamellar Widmastaetten structure drives to the bending of plates (Fig. 9a) during machinery operations. This plasticity provokes a superficial micro roughness creating a notch effect (Fig. 9b). The combined effect of micro-roughness and the plates in the grain bound- aries makes a decrease in the fatigue properties of the alloy.

Fatigue properties after sintering (endurance limit 483 MPa) are also minor than previous fatigue properties, the material exhibited just before sintering treatment (endurance limit 690 MPa). The endurance limit can be improved by BUS heat treatment to 621 MPa.

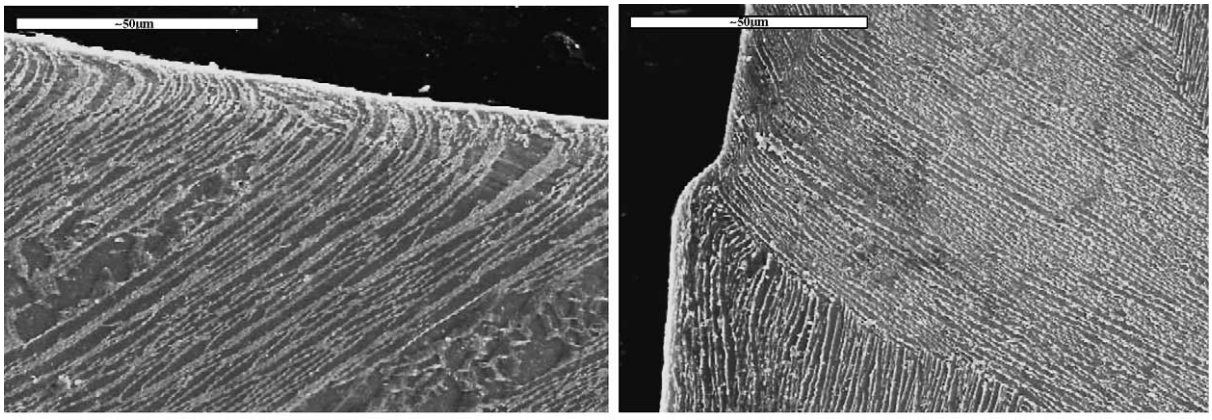

Fig. 9. (a) Plasticity of the surface: bended Widmastaetten plates. (b) Micro roughness due to plasticity plus a-plates notch effect.

Thus, it is convenient to procure to the prosthesis, treatments conducting to minimise the effects of the indicated microstructural changes, increasing the endurance limit. These treatments must lead to break big Windmastaetten plates.

Conclusions

The conclusions reached in this study are as follows:

- Sintering process produce a very important grain size increase, especially in the inner areas on the piece.
- The grain size enlargement and Widmastaetten plates formation after the beads sintering process, decreases the mechanical properties and fatigue properties of the material, but microhardness remains constant.
- Post-sinter treatments break the large Widmastaetten plates formed into acicular structure.
- The breakage of large Widmastaetten plates lightly increases the mechanical properties mainly the fatigue properties.

Acknowledgements

The authors wish to thank the Bio-Vac Espan˜a, S.A., for its contribution with the materials and the thermal treatments performed. They are also grateful to the Electronic Microscopy Service of the Politechnical University of Valencia (UPV), where microstructure study was done.

References

[1] C.A. Engh, J. Bone Joint Surg. Am. B 69 (1987) 45.

[2] J.D. Bobyn, et al., Adv. Orthop. Surg. (1983) 137.

[3] A.F. Brooker, et al., J. Bone Joint Surg. Am. A 66 (1986) 619.

[4] J.P. Hooten, et al., J. Bone Joint Surg. Am. A 77 (1995) 903.

[5] R.M. Pilliar, et al., Clin. Orthop. Relat. R. 150 (1980) 263.

[6] J.D. Bobyn, et al., Clin. Orthop. Relat. R. 149 (1980) 291.

[7] R.M. Pilliar, Clin. Orthop. Relat. R. 176 (1983) 42.

[8] F.J. Gil, J.A. Planell, Scripta Mater. 25 (1991) 2843.

[9] Bio-Vac Inc. Evaluation of the BUS heat treatment for sintered Ti–6Al–4V alloy, Technical Report, MI, USA, 1990.

[10] ASTM F 136-98, Standard specification for wrought Ti–6Al–4V ELI (extra low interstitial) alloy (UNS R56401) for surgical implants applications.

[11] International standard ISO 5832-3, Implants for surgery—metallic materials. Part 3. Wrought Ti–6Al–4V alloy, 1990.

[12] ASTM F 1580-95. Standard specification for titanium and Ti–6Al– 4V alloy powders for coating of surgical implants.

[13] ASTM F 67-95, Standard specification for unalloyed for surgical implants applications.